Accelerated Publications

Conformational Dimorphism and Transmembrane Orientation of Prion Protein Residues 110−136 in Bicelles†

Kerney Jebrell Glover, Jennifer A. Whiles, Matthew J. Wood, Giuseppe Melacini, Elizabeth A. Komives,* and Regitze R. Vold

Department of Chemistry and Biochemistry, 0359, University of California at San Diego, 9500 Gilman Drive, La Jolla, California 92093-0359

Received July 17, 2001; Revised Manuscript Received September 12, 2001

ABSTRACT: A fragment corresponding to the putative membrane-associating domain of the prion protein (residues 110−136) was analyzed in phospholipid bicelles. Prion(110−136) associated with bicelles and exhibited a lipid- and pH-dependent conformational dimorphism between unstructured (pH 4.5) and α-helical (pH 7.5). Mutational analysis indicated that the charge state of a single histidine residue was largely responsible for the dimorphism. Amide−lipid NOEs and amide−water chemical exchange measurements revealed that the helical conformation of prion(110−136) spanned the bilayer, and were corroborated by solid-state deuterium NMR experiments indicating that the helical axis rested at a 16° angle with respect to the bilayer normal.

The prion protein is a 35 kDa glycoprotein which has been implicated in a variety of neurodegenerative diseases, including Creutzfeldt-Jakob disease, Gerstmann-Straussler-Scheinker disease, and bovine spongiform encephalopathy (*1*). Even though the normal function of the prion protein is unknown, neurodegenerative disease has been implicated in the buildup of an abnormal isoform (PrP^{Sc}) in the brain (*1*). Furthermore, PrP^{Sc} is thought to facilitate the conversion of normal prion (PrP^{C}), which is protease-sensitive, to PrP^{Sc} which has a higher β-sheet content and is protease-resistant (*2*). Although most prion molecules are attached to the membrane by a glycolipid anchor, two transmembrane isoforms of the prion protein have been identified in the ER[1] (*3*). Interestingly, the two isoforms appear to span the membrane at the same residues, 110−135, but pass through in different directions (*3*). In particular, the isoform in which the C-terminus resides in the lumen of the ER (^{Ctm}PrP) has been proposed as another key player in the transmission of prion disease (*3*). More recently, ^{Ctm}PrP has been shown to have a glycolipid anchor in addition to its transmembrane segment (*4*).

To investigate the behavior of this region in the presence of a phospholipid bilayer, we studied the peptide corresponding to residues 110−136 (Ac-KHMAGAAAAGAVVGGLGGYMLGSAMSR-NH_2) in phospholipid bicelles. This peptide lacks the high number of hydrophobic residues (Ile, Leu, Val, and Phe), and is more soluble than typical transmembrane domains (*5*). Therefore, on the basis of its sequence, it is difficult to predict if and how it will associate with a membrane.

Bicelles are discoidal lipid aggregates comprised of two types of phospholipids: DMPC and DHPC. The long chain lipids (DMPC) form a nativelike planar bilayer in the center of the bicelle, while the short chain lipids (DHPC) occupy the rim where they shield the long chain lipid tails from water (*6*). In addition, bicelles possess a unique phase behavior which allows for studies under both aligned and unaligned conditions (*7*, *8*). Aligned conditions allow for the examination of peptide and lipid order using solid-state NMR techniques, while unaligned conditions are suitable for high-resolution solution NMR techniques as well as other solution spectroscopies. On the basis of the size of unaligned bicelles, a very long correlation time (170 ns) is predicted and consequently poor NMR line widths (*8*). However, previous studies have shown that peptides tightly associated with the bicelle have suitable line widths, and T_2 values of ∼15 (*8*, *9*). This is likely due to the high degree of motion of the lipid molecules (*8*). Our measurements indicate that prion(110−136) binds to bicelles, and spans the bilayer as an α-helix at pH 7.5. At lower pH, prion(110−136) becomes predominantly unstructured. Mutational analysis revealed that this conformational dimorphism was due to the charge state of a single histidine residue located near the N-terminus.

MATERIALS AND METHODS

Materials. Isotopically labeled amino acids and deuterium-depleted water were purchased from Cambrige Isotopes

† Research supported by NIH Grant 5 R01 GM54034 and NSF Grant CHE9632618 to R.R.V. K.J.G. acknowledges training support from the National Institutes of Health.

* To whom correspondence should be addressed. Telephone: (858) 534-3058. Fax: (858) 534-6174. E-mail: ekomives@ucsd.edu.

[1] Abbreviations: NOE, nuclear Overhauser effect; NMR, nuclear magnetic resonance; ER, endoplasmic reticulum; DMPC, 1,2-dimyristoyl-*sn*-glycero-3-phosphocholine; DHPC, 1,2-dicaproyl-*sn*-glycrero-3 phosphocholine; NBD, 7-nitrobenz-2-oxa-1,3-diazole; NOESY, nuclear Overhauser effect spectroscopy; FHSQC, fast heteronuclear single-quantum coherence; MALDI-TOF, matrix-assisted laser desorption ionization time-of-flight.

10.1021/bi011485m CCC: $20.00
Published on Web 10/13/2001

Laboratories (Cambridge, MA). DMPC, DHPC, and their chain-perdeuterated counterparts (DMPC-d_{54} and DHPC-d_{22}) were purchased from Avanti Polar Lipids (Alabaster, AL).

Peptide Synthesis and Purification. Peptides were prepared according to previously published methods using isotopically labeled amino acids (*5*). The fluorescently tagged peptide was labeled at the N-terminus with a NBD moiety (*10*). The crude peptide was purified by reverse phase high-performance liquid chromatography using a Phenomenex Jupiter C4 column and a linear gradient from 80% water and 20% acetic acid to 80% 1-butanol and 20% acetic acid. Peptide purity was verified by MALDI-TOF mass spectrometry.

Although previous studies showed that the transmembrane domain of the prion protein encompassed residues 110−135 (*3*), we felt that the full transmembrane domain was encompassed in residues 110−136 which added an additional Arg residue at the C-terminus. Furthermore, positively charged residues located at the ends of transmembrane helices have been postulated to play an important role in membrane stabilization by interacting with the phospholipid headgroups (*11*).

Sample Preparation. Bicellar samples were prepared by dissolving the peptide in water (deuterium-depleted water was used for solid-state samples) and D_2O (omitted in solid-state samples), adding DMPC or DMPC-d_{54}, and vortexing until a homogeneous suspension was obtained. Next, a 25% (w/w) solution of DHPC or DHPC-d_{22} in water was added, and the solution was vortexed until it was clear. Last, 1 M buffer (acetate for pH 4.5, MES for pH 6.0, and HEPES for pH 7.5) was added followed by mixing and mild centrifugation to remove bubbles from samples. For solution NMR samples, final concentrations of constituents in the samples were 15% (w/w) total lipid (0.5 DMPC:DHPC molar ratio), 5% (v/v) D_2O, 25 mM buffer, and a 1:100 peptide:DMPC ratio. For solid-state samples, final concentrations of constituents in the samples were 15% (w/w) total lipid (3.5 DMPC:DHPC molar ratio), 25 mM buffer, and a 1:50 peptide:DMPC ratio. For circular dichroism and fluorescence samples, final concentrations of constituents in the samples were 4% (w/w) total lipid (0.5 DMPC:DHPC molar ratio), 5 mM buffer, and a 1:100 peptide:DMPC ratio.

Fluorescence Spectroscopy. Spectra were obtained at 37 °C on a Perkin-Elmer LB50B luminescence spectrometer using an excitation wavelength of 468 nm.

Circular Dichroism Spectroscopy. Spectra were obtained at 37 °C on an Aviv circular dichroism model 202 spectrometer.

Solution NMR Spectroscopy. All NMR experiments were carried out at 37 °C on a Bruker DRX-600 NMR spectrometer operating at a ^{1}H resonance frequency of 600.13 MHz and equipped with pulsed field *x*,*y*,*z*-gradients. Amide−lipid NOEs were measured using a NOESY experiment in which a double band-selective pulsed field gradient spin echo was inserted after the NOE mixing period and prior to acquisition (*12*). Specifically, a phase-modulated 1.8 ms REBURP pulse was used for selection of a frequency band centered at 3.10 ppm (*13*). FHSQC experiments were used to observe secondary structural changes with pH (*14*). Amide−water chemical exchange was monitored using a two-dimensional NOESY-FHSQC experiment (τ_{mix} = 90 ms) (*15*). In all NOESY-type experiments, an interscan repetition delay of 2 s was used to allow for the recovery of the lipid and water magnetizations. The $\{^1H\}-^{15}N$ steady-state NOEs were determined as previously described (*9*). Data sets were processed using Felix 97.0 (Molecular Simulations) with a 90°-shifted squared sine-bell apodization and zero filling by a factor of 2, prior to Fourier transformation and phase correction.

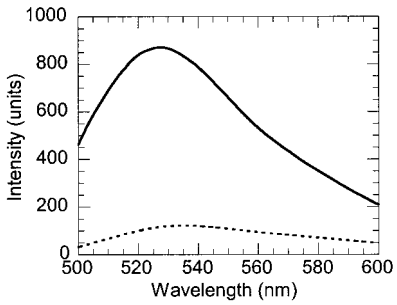

FIGURE 1: Fluorescence emission spectra of prion(110−136) with an N-terminal NBD moiety (pH 4.5). The solid line is for a bicellar solution and the dotted line for water.

Solid-State ^{2}H NMR Spectroscopy. Deuterium quadrupole-echo spectra were acquired at 55.3 MHz using a Chemagnetics CMX-250/360 spectrometer as previously described (*9*). Data processing included fractional left shifting, zero filling, and multiplication by an exponential (25 and 500 Hz line broadening for lipid and peptide spectra, respectively) of the second half of the quadrupole echo prior to Fourier transformation.

RESULTS AND DISCUSSION

Prion(110−136) Binds to Membranes. To assess the affinity of binding of prion(110−136) to phospholipid bicelles, we used a peptide that was tagged with a NBD moiety at the N-terminus. In water, the fluorescence emission maximum was 536 nm and the intensity was low. In the prescence of bicelles, the emission maximum was blue-shifted to 527 nm and the intensity increased dramatically (Figure 1), revealing that the peptide was in a more apolar environment. The emission maximum remained constant even when the bicelle concentration was increased by 5-fold or decreased by 2-fold, indicating that the peptide was completely bound. Moreover, peptide binding was not dependent on pH (from 4.5 to 7.5) as both the intensity and the emission maximum remained constant.

The interactions between the peptide and the bicelle were further investigated using amide−lipid NOEs from band-selective NOESY spectra at pH 7.5 (*16*). Experiments in which either one or both phospholipids were chain perdeuterated allowed us to disentangle which NOEs were due to amide−peptide, amide−rim, and amide−planar region interactions (Figure 2). The absence of NOEs arising from the DHPC when compared to the presence of NOEs from the DMPC confirmed that prion(110−136) was associated primarily with the planar region which is the more biologically relevant portion of the bicelle. Similarly, at pH 4.5, NOEs were observed *only* to DMPC. However, the signals were less disperse, and the NOEs to the aromatic ring protons were very weak. This is consistent with the fluorescence experiments which indicated that prion(110−136) was bound to the bicelles at both high and low pH.

Prion(110−136) Adopts a Transmembrane Orientation. To probe the solvent accessibility of prion(110−136),

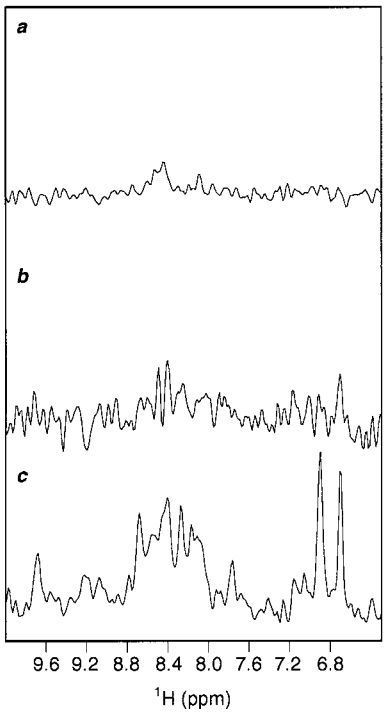

FIGURE 2: One-dimensional horizontal slices taken at 1.31 ppm (resonance frequency which contains contributions from the methylene protons of the lipid chains) from various band-selective NOESY spectra of prion(110−136) (1.0 mM). (a) Bicelles prepared with DMPC-d_{54} and DHPC-d_{22} (amide−peptide cross-peaks). (b) Bicelles prepared with DMPC-d_{54} and DHPC [amide−rim cross-peaks, spectrum acquired with 2.88 times as many scans to equalize the intensity discrepancy arising from differences in the number of methylenes between DMPC and DHPC as well as differences in the concentrations of the two lipids (twice as much DHPC as DMPC)]. (c) Bicelles prepared with DMPC and DHPC-d_{22} (amide−planar region cross-peaks). Spectrum ***a*** was subtracted from spectra ***b*** and ***c*** to eliminate contributions from amide−peptide cross-peaks.

Table 1: Values for Glycine Residues in an α-Helical Conformation (pH 7.5)

residue	^{1}H chemical shift (ppm)	^{15}N chemical shift (ppm)	{^{1}H}−^{15}N heteronuclear NOE	theoretical ratio (^{15}N:$^{14+15}$N)[a]	observed ratio (^{15}N:$^{14+15}$N)[a]
114	8.59	104.57	0.36 ± 0.06	0.15	0.17
119	8.55	103.05	0.79 ± 0.16	0.25	0.24
123	9.20	105.63	0.81 ± 0.24	0.40	0.44
124	8.69	110.66	0.78 ± 0.08	0.55	0.50
126	8.44	104.57	0.84 ± 0.04	0.70	0.72
127	9.68	108.91	0.73 ± 0.23	0.85	0.83
131	9.05	106.68	0.71 ± 0.06	1.0	1.0

[a] A peptide was prepared in which each glycine residue contained a different ^{15}N:$^{14+15}$N ratio. An HSQC of this peptide was compared to another peptide in which each glycine residue had a ^{15}N:$^{14+15}$N ratio of 1. The observed ratios were obtained by taking the ratio of the intensity of the peaks in the partially ^{15}N-labeled peptide to that of the uniformly labeled peptide. Each residue fell within ±0.05 of its theoretical ratio.

amide−water chemical exchange cross-peaks were analyzed at pH 7.5 for each of the glycine residues which were assigned using a strategy based on varying the percentage of ^{15}N (Table 1) (*17*). A ^{15}N-edited NOESY-FHSQC spectrum showed that all of the glycine residues had an amide−lipid NOE, but only a very weak amide−water chemical exchange cross-peak. This indicated that the peptide was likely in a transmembrane configuration with the glycine residues located in the solvent inaccessible hydrophobic core of the membrane.

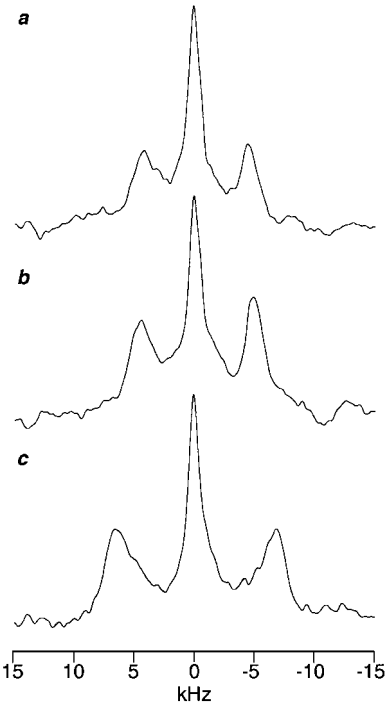

FIGURE 3: Quadrupolar splittings of prion peptides in aligned bicelles: (a) A117-d_3, (b) A118-d_3, and (c) A120-d_3.

To obtain the orientation of prion(110−136) at pH 7.5 with respect to the bilayer, solid-state deuterium NMR in aligned bicelles was carried out on three separately labeled peptides (A117-d_3, A118-d_3, and A120-d_3) (*9*, *18*). Solid-state ^{2}H lipid spectra of both chain-perdeuterated DMPC and DHPC confirmed that the bicelles remained well-aligned and stable in the presence of peptide, while a circular dichroism spectrum revealed that prion(110−136) was highly α-helical (Figure 5b) (*19*). Furthermore, high heteronuclear NOE values for the glycine residues (Table 1) showed that the helix was conformationally stable (*9*). The quadrupolar splitting obtained from each peptide (Figure 3 and Table 2) was matched with possible peptide tilt angles using a program written in house (*9*). Since the resultant C−D bond vector lies at a 56° angle with respect to the helical axis in the case of Ala-d_3 residues, the observed quadrupolar splitting depends not only on the tilt but also on the specific rotation of the peptide in the bilayer. Motional averaging about the helical axis is excluded because it would collapse the splittings to ∼0 kHz (*18*). The only tilt angle consistent with all three labels was 16° with respect to the bilayer normal, which is consistent with a membrane-spanning orientation, and matches the results obtained from the solvent accessibility studies. In addition, this orientation was consistent with molecular modeling studies of prion protein residues 105−132 in which transmembrane insertion was predicted (*20*).

Table 2: Quadrupolar Splittings of Prion(110−136) in Aligned Bicelles

residue	splitting (kHz)
A117	8.2 ± 1.5
A118	8.7 ± 1.5
A120	12.6 ± 1.5

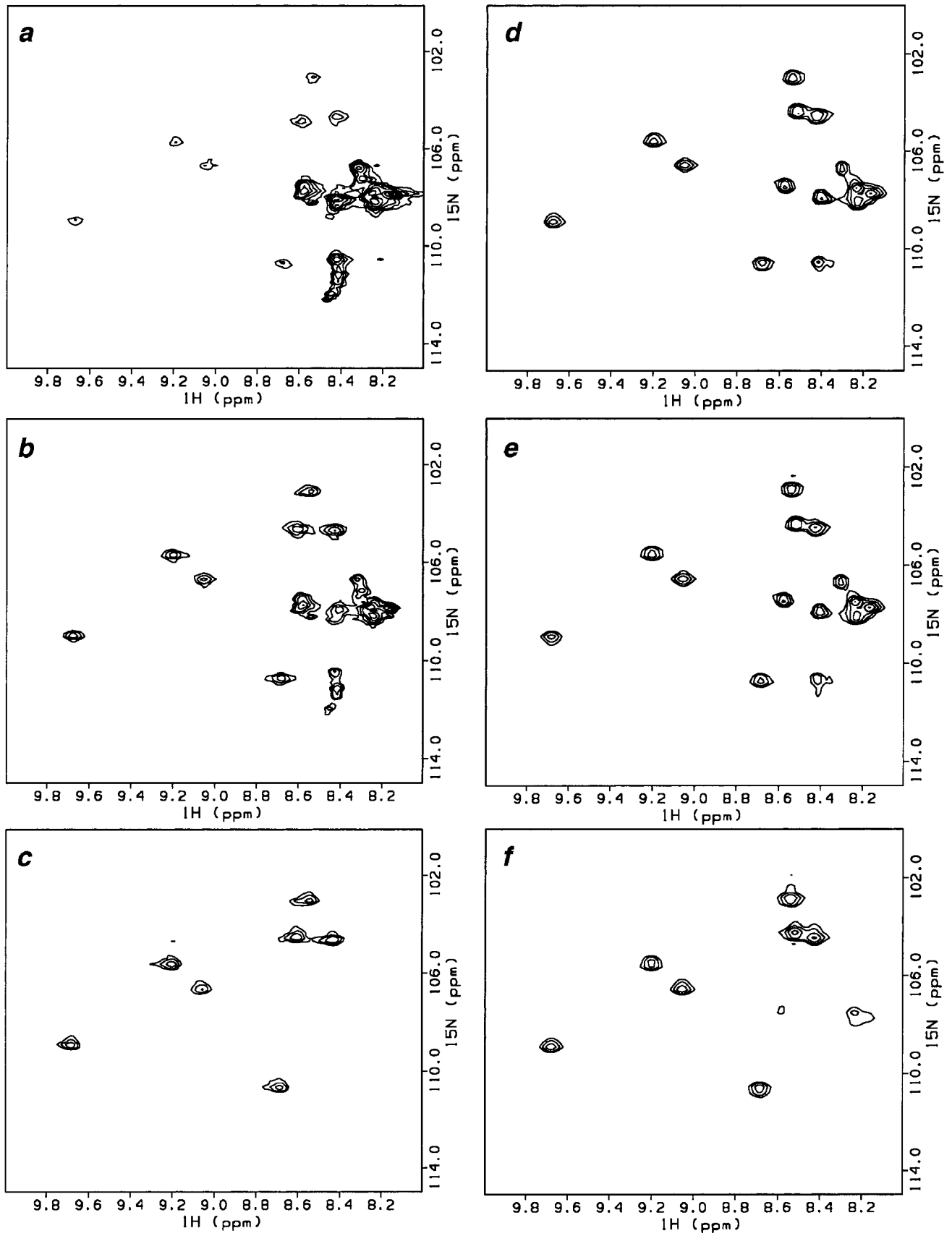

FIGURE 4: FHSQC spectra of prion peptides in bicelles with each of its seven glycines labeled with ^{15}N: (a) prion(110−136) at pH 4.5, (b) prion(110−136) at pH 6.0, (c) prion(110−136) at pH 7.5, (d) prion(110−136) His111Gln at pH 4.5, (e) prion(110−136) His111Gln at pH 6.0, and (f) prion(110−136) His111Gln at pH 7.5.

Lipid- and pH-Dependent Reversible Conformational Change. The HSQC spectrum of prion(110−136) in bicelles at pH 4.5 showed mainly random coil chemical shift values (Figure 4a) (*21*). There was, however, a second set of well-

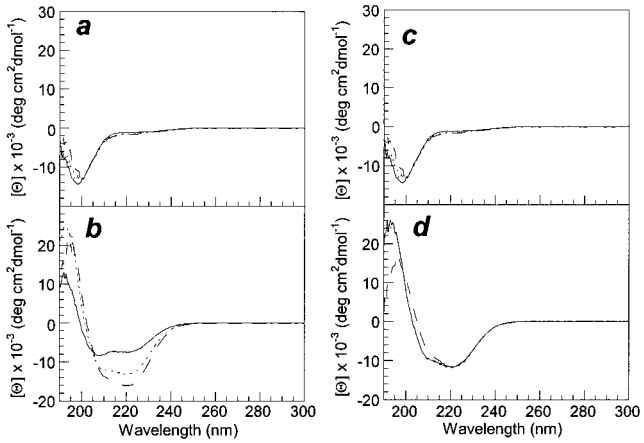

FIGURE 5: Circular dichroism spectra of prion peptides: (a) prion(110−136) in water, (b) prion(110−136) in bicelles (c) prion(110−136) His111Gln in water, and (d) prion(110−136) His111Gln in bicelles. The solid line is for pH 4.5, the dotted line for pH 6.0, and the dashed line for pH 7.5.

dispersed weak resonances indicative of a structured conformation. When the pH was increased to 6.0 (Figure 4b) and then to 7.5 (Figure 4c), the intensity of the well-dispersed chemical shifts increased dramatically along with a concomitant decrease in the intensity of the random coil resonances. Although circular dichroism spectra (Figure 5a) showed that the peptide was unstructured at all three pHs in aqueous solution, in the presence of bicelles (Figure 5b) a dramatic increase in the α-helical content with increasing pH was observed. At pH 4.5, there was a small population of apparently helical conformers consistent with the weak signals observed in the HSQC spectrum (Figure 4a). Thus, prion(110−136) exhibited a pH-dependent conformational dimorphism from predominantly unstructured to predominantly α-helical *only* in the presence of a lipid environment. This conformational dimorphism was independent of the peptide:DMPC ratio when it was varied from 1:200 to 1:50. While not definitive, the lack of concentration dependence suggests that it is the peptide−lipid interaction, rather than oligomerization, that is driving structure formation.

Mutational Analysis. Since the conformational change occurred around the pK_a of a histidine side chain, we postulated that His111 may play an important role in the conformation of prion(110−136). Figure 5c shows that the His111Gln mutant is unstructured in water at all three pHs, but shows an α-helical structure at all pHs in the presence of bicelles (Figure 5d). Importantly, the helical content of the mutant, unlike that of the wild type, is *not* pH-dependent. This is corroborated by HSQC spectra of the His111Gln mutant (Figure 4d−f) which show that the intensity of the α-helical resonances does *not* change with pH. A small quantity of signal at the random coil chemical shift is present, and decreases in intensity at pH 7.5. We attribute this to the higher amide−chemical exchange rates and buffer conditions at this pH, particularly in view of the unchanging circular dichroism spectra (Figure 5d). Similar results were observed for a His111Phe mutant. Since His111 is located near the N-terminus, the strong structural effects of the His111 charge state are likely due to the interaction between the charge on the histidine and the helix dipole (*22*). At low pH, the positive charge on His111 interacts destructively with the helix dipole, destabilizing the helical structure.

CONCLUSIONS

We have shown that prion(110−136) binds to lipid bilayers, and exhibits a reversible conformational change from a predominantly unstructured form at pH 4.5 to a predominantly α-helical form at pH 7.5. Furthermore, when in an α-helical conformation, prion(110−136) adopts a transmembrane orientation. The presence of a helical conformation for prion(110−136) is notable considering the high number of "structure-breaking" glycine residues, and accentuates the powerful role that lipid interactions can play in protein structure. Furthermore, the dependence of the prion(110−136) conformation on the charge state of one histidine residue reveals that a single amino acid can dictate peptide structure. Taken together, these results suggest that the conformation of the prion protein may be highly dependent upon the cellular compartment in which it resides. In fact, the observed lipid association, conformational dimorphism, and transmembrane orientation observed in the prion(110−136) help to support the membrane disposition observed for the prion protein as a whole. In addition, the induction of a transmembrane helical conformation as a result of the deprotonation of His111 is consistent with the increased levels of transmembrane prion protein found for the Lys110Ile/His111Ile double mutant (*3*, *4*, *23*).

ACKNOWLEDGMENT

We thank Dr. Yitzhak Tor and Dr. Susan Taylor for use of their instruments, Dr. John Wright, Steven Berkus, Akilah Weber, and Mark Lillig for laboratory assistance, and Paul Martini for computer program development.

REFERENCES

1. Prusiner, S. B. (1998) *Proc. Natl. Acad. Sci. U.S.A. 95*, 13363−13383.
2. Kocisko, D. A., Come, J. H., Priola, S. A., Chesebro, B., Raymond, G. J., Lansbury, P. T., and Caughey, B. (1994) *Nature 370*, 471−474.
3. Hegde, R. S., Mastrianni, J. A., Scott, M. R., DeFea, K. A., Tremblay, P., Torchia, M., DeArmond, S. J., Prusiner, S. B., and Lingappa, V. R. (1998) *Science 279*, 827−834.
4. Stewart, R. S., and Harris, D. A. (2001) *J. Biol. Chem. 276*, 2212−2220.
5. Glover, K. J., Martini, P. M., Vold, R. R., and Komives, E. A. (1999) *Anal. Biochem. 272*, 270−274.
6. Sanders, C. R., and Prosser, R. S. (1998) *Structure 6*, 1227−1234.
7. Sanders, C. R., Hare, B. J., Howard, K. P., and Prestegard, J. H. (1994) *Prog. NMR Spectrosc. 26*, 421−444.
8. Vold, R. R., Prosser, R. S., and Deese, A. J. (1997) *J. Biomol. NMR 9*, 329−335.
9. Whiles, J. A., Brasseur, R., Glover, K. J., Melacini, G., Komives, E. A., and Vold, R. R. (2001) *Biophys. J. 80*, 280−293.
10. Rapaport, D., and Shai, Y. (1991) *J. Biol. Chem. 266*, 23769−23775.
11. Webb, R. J., East, J. M., Sharma, R. P., and Lee, A. G. (1998) *Biochemistry 37*, 673−679.
12. Dalvit, C. (1999) *J. Biomol. NMR 11*, 437−444.
13. Geen, H., and Freeman, R. J. (1991) *J. Magn. Reson. 93*, 93−141.
14. Mori, S., Abeygunawardana, C., Johnson, M. O., and Van Zijl, P. C. M. (1995) *J. Magn. Reson., Ser. B 108*, 94−98.
15. Huster, D., and Gawrisch, K. (1999) *J. Am. Chem. Soc. 121*, 1992−1993.
16. Seigneuret, M., and Levy, D. (1995) *J. Biomol. NMR 5*, 345−352.

17. Ikura, M., Krinks, M., Torchia, D. A., and Bax, A. (1990) *FEBS Lett. 266*, 155−158.
18. Jones, D. H., Barber, K. R., VanDerLoo, E. W., and Grant, C. W. M. (1998) *Biochemistry 37*, 16780−16787.
19. Vold, R. R., and Prosser, R. S. (1996) *J. Magn. Reson., Ser. B 113*, 267−271.
20. Haïk, S., Peyrin, J. M., Lins, L., Rosseneu, M. Y., Brasseur, R., Langeveld, J. P., Tagliavini, F., Deslys, J. P., Lasmèzas, C., and Dormont, D. (2000) *Neurobiol. Dis. 7*, 644−656.
21. Wuthrich, K. (1986) *NMR of Proteins, and Nucleic Acids*, John Wiley and Sons, New York.
22. Armstrong, K. M., and Baldwin, R. L. (1993) *Proc. Natl. Acad. Sci. U.S.A. 90*, 11337−11340.
23. Lopez, C. D., Yost, C. S., Prusiner, S. B., Myers, R. M., and Lingappa, V. R. (1990) *Science 248*, 226−229.

BI011485M